Microchemical Journal 196 (2024) 109685

Contents lists available at ScienceDirect

Microchemical Journal

journal homepage: www.elsevier.com/locate/microc

Silver nanocluster-based colorimetric/fluorimetric dual-mode sensor for the detection of bromide and sulfite in waters and wastewaters

Nerea Villarino, Isela Lavilla, Francisco Pena-Pereira *, Carlos Bendicho *

Centro de Investigación Mariña, Universidade de Vigo, Departamento de Química Analítica e alimentaria, Grupo QA2, Edificio CC Experimentais, Campus de Vigo, As Lagoas, Marcosende 36310 Vigo, Spain

ARTICLE INFO

Keywords:
Bromide
Dual sensor
Microextraction
Silver nanoclusters
Smartphone-based detection
Sulfite

ABSTRACT

In this work, the development of a fluorimetric/colorimetric dual-mode nanosensor for the determination of sulfite and fluorimetric determination of bromide involving silver nanoclusters (AgNCs) is reported. SO_2 and Br_2 were found to significantly modify the optical properties of AgNCs. Particularly, both volatiles weakened the fluorescence of AgNCs, whereas a color change from nearly colorless to yellowish/brown occurred upon exposure of AgNCs to SO_2. Accordingly, three smartphone-based optical assays were devised for sulfite and bromide determination, involving *in situ* volatile generation and enrichment/trapping of the selectively formed volatiles by AgNCs confined in a droplet and exposed to the headspace above the sample. A hydrophobized cellulose substrate acting as drop holder enabled integrating both the enrichment and the subsequent smartphone-based optical detection in a straightforward manner. Smartphone-based digitization of the enriched AgNCs microdrops and subsequent image processing using a smartphone and its integrated App, respectively, were used for quantitative purposes. Under optimal conditions, limits of detection (LODs) of 1.1 μM and 1.5 μM were achieved for the fluorimetric determination of sulfite and bromide, respectively, whereas sulfite was alternatively determined by colorimetric readout, yielding a LOD of 37.0 μM. The repeatability, expressed as relative standard deviation, was found to be in the range of 5.1–5.9 % in all cases (N = 8). The applicability of the method was demonstrated in aqueous samples of increasing complexity, with recoveries in the range 91–109 %. In addition, the responsiveness of AgNCs to SO_2 and Br_2 rendered them suitable for the monitoring of bromide and sulfite in increasingly relevant advanced reduction processes such as the UV/sulfite system, as demonstrated in this work.

1. Introduction

Bromide is the most significant precursor of bromate and some other bromo-organic products included under the denomination of disinfection by-products (DBPs). Hundreds of brominated DBPs have been detected in treated wastewaters, associated to their unintentional *in situ* formation in widely used disinfection processes such as ozonation or chlorination [1,2]. Even though bromate is regulated by several agencies [3], the vast majority of brominated DBPs are not included in the regulations. Moreover, many of brominated DBPs are yet to be identified, thus preventing their monitoring in natural waters and wastewaters. In this regard, several control strategies have been recently proposed to minimize the formation of brominated DBPs, including the monitoring of bromide in waters due to its key role as a DBPs precursor [4].

Sulfur dioxide emissions associated to industrial processes lead to the formation of sulfite, which is harmful to natural resources and human health, causing acid rain and reducing the water quality [5]. Sulfiting agents are also widely used in the food industry as antioxidants or preservatives. In spite of this, several health issues have been associated to sulfite, including asthma, dermatitis or bronchoconstriction [6]. In addition, both the EU Regulation No 1169/2011 and the Codex Alimentarius classify sulfites as substances causing allergies or intolerances [7,8]. On the other hand, increasing attention is being paid to the use of sulfite in both advanced oxidation and reduction processes for degradation of pollutants in water [9]. Remarkably, bromide-containing water treatment can be performed by sulfite-based advanced oxidation processes (AOPs) without involving bromate formation, unlike conventional AOPs. In addition, sulfite/UV advanced reduction processes (ARPs) are increasingly being employed for degradation of bromate, among other pollutants, based on the reducing capacity of sulfite radicals, hydrogen radicals and hydrated electrons formed by exposure of

* Corresponding authors.
E-mail addresses: fjpena@uvigo.es (F. Pena-Pereira), bendicho@uvigo.es (C. Bendicho).

https://doi.org/10.1016/j.microc.2023.109685
Received 15 August 2023; Received in revised form 27 October 2023; Accepted 19 November 2023
Available online 21 November 2023

sulfite to UV irradiation [9].

A number of methods have been reported in the literature for the determination of bromide and sulfite in water and wastewater samples. Standard methods for the determination of bromide in waters include the phenol red colorimetric method, applied both in batch and flow systems, and preferably, ion chromatography and capillary electrophoresis [10]. Regarding the determination of sulfite in waters, standard methods include the iodometric titration and the phenanthroline-based colorimetric methods [10]. Several alternative methodologies have been proposed for bromide and sulfite determination, involving spectrometric, chromatographic and electroanalytical techniques [11–21]. Even though these methods are suitable for the analysis of aqueous matrices, they commonly require relatively expensive and hardly portable analytical instrumentation and skilled operators. In this vein, a great deal of interest is placed nowadays in the development of cost-effective, portable and fast alternatives for on-site analysis.

In recent years, the combination of paper-based analytical devices (PADs) with everyday information and communication technology (ICTs) devices has reached a great popularity for detection purposes [22–24]. In sensing devices, PADs commonly exploit the porosity and hydrophilic nature of cellulose for the immobilization of responsive materials so that optical and electrochemical transduction can be implemented. Single-mode detection is most applied with PADs, even though there is great interest in the development of sensors with dual-signal readouts since mutual verification is attained, thus increasing the reliability of assays [25]. PADs have also been combined with headspace microextraction for detecting volatile compounds [26–28]. Alternatively, hydrophobized cellulose substrates have been proposed as highly convenient holders for integrating in-drop enrichment and sensing of volatiles without requiring additional drop manipulation, leading to improved sensitivity when compared with hydrophilic PADs [29,30]. The development of non-instrumental dual-mode sensing approaches involving PADs is thus particularly valuable. However, the number of contributions involving PADs for volatile sensing with dual-mode detection is still limited [26,31–33] and, to the best of our knowledge, droplet-based assays with dual-signal readouts have not been reported in the literature.

Metallic nanoclusters are luminescent materials with particle sizes in the range 1 to 3 nm that exhibit fascinating properties between those of molecules and larger nanoparticles. They display favorable photostability, water solubility, high emission rates, and can be easily prepared. Particularly, the unique characteristics of AgNCs make them appealing in various fields, with special emphasis on their application in sensing devices [34–37]. However, their performance as nanoprobes can be affected by the presence of matrix components and/or the chemicals required for accomplishing the assay. This constraint could be minimized or avoided by a rationale combination of confined luminescent materials with *in situ* formation of volatiles [26] and, interestingly, this approach would allow volatile sensing involving AgNCs, a largely underexplored direction [36].

Therefore, the aim of this work is the development of smartphone-based fluorimetric and/or colorimetric assays based on AgNCs for the selective determination of sulfite and bromide in aqueous matrices. To the best of our knowledge, this work constitutes the first report devoted to the determination of sulfite and bromide using a single optical nanosensor.

2. Experimental

2.1. Reagents and materials

All reagents were of analytical reagent grade. High-purity deionized water obtained by a Millipore Sigma Simplicity ultrapure water system (Millipore Iberian S.A., Madrid, Spain) was used. Polyethyleneimine (PEI), 4-(2-hydroxyethyl)-1-piperazineethanesulfonic acid (HEPES) and silver nitrate from Sigma-Aldrich (St. Louis, MO, USA) and formaldehyde 39 % (w/v) from AnalaR Normapur (Leuven, Belgium) were used to synthesize AgNCs. Standard solutions of sulfite and bromide were prepared from sodium sulfite (Probus, Badalona, Spain) and potassium bromide (Sigma-Aldrich, St. Louis, MO, USA), respectively. The following reagents were also used: Hydrochloric acid 37 % (w/w) from AnalaR Normapur, potassium bromate, ethylenediaminetetraacetic acid (EDTA), zinc sulfate, copper sulfate, nickel chloride, potassium nitrate, ammonium nitrate and chloramine-T from Probus (Badalona, Spain), iron sulfate and sodium selenite from Sigma-Aldrich (St. Louis, MO, USA), cobalt chloride, manganese chloride and ammonium heptamolybdate from Scharlau (Barcelona, Spain), boric acid and calcium chloride from Prolabo (Paris, France), magnesium nitrate, potassium dihydrogen phosphate and potassium hydrogen phthalate from Merck (Darmstadt, Germany).

1,10-phenantroline and octyl alcohol from Merck, ferric ammonium sulfate and sulfamic acid from Panreac (Barcelona, Spain) and ammonium bifluoride from Probus were used for the determination of bromide and sulfite by the reference methods.

Whatman 1PS Phase Separator (Maidstone, Kent, UK), a filter paper impregnated with a stabilized silicone, was used as drop holder for both extraction and smartphone-based image acquisition.

2.2. Apparatus

A Samsung Galaxy A70 smartphone (Samsung, Seoul, South Korea), a C-10 Chromato-Vue mini-UV viewing cabinet (Analytik Jena, Jena, Germany) equipped with a 254/365 nm UV lamp (The Science Company, Lakewood, CO, USA) and a portable PULUZ photo studio lightbox (Shenzhen PULUZ Technology Limited, Shenzhen, China) with 20 LEDs were used for digitization of AgNCs drops. RGB Color Detector App (The Programmer, Google Play Store) and ImageJ, a free image analysis program [38], were employed to processing the digital images for acquisition of analytical responses. Statgraphics Centurion XVI.I software (StatPoint Technologies, Warrengton, VA, USA) was used for the optimization of experimental parameters.

A Horiba Fluoromax-4 spectrofluorometer (Horiba Scientific, Edinson NJ, Tokyo, Japan), a Thermo Scientific Nanodrop ND-1000 microvolume UV − vis spectrophotometer (Wilmington, DE, USA), a Thermo Scientific Nanodrop Model ND-3300 fluorospectrometer (Thermo Scientific, Wilmington, DE, USA), a JEOL JEM-2010 (200 kV) and JEOL JEM 1400F (120 kV) transmission electron microscopes (Tokyo, Japan), and a Thermo Scientific NEXSA X-Ray Photoelectron Spectrometer (XPS) instrument (Waltham, USA) equipped with aluminum Kα monochromatized radiation at 1486.6 eV X-ray source were used for the characterization of AgNCs in the absence and presence of *in situ* formed SO_2 and Br_2. In addition, a 705 UV Digester system (Metrohm, Herisau, Switzerland) equipped with a high-pressure mercury lamp (500 w) was used to carry out the UV/sulfite process.

A 940 Professional IC Vario ion chromatograph equipped with a conductivity detector and a Metrosep A Supp 5–250/4.0 column (Metrohm, Schweiz AG, Switzerland) thermostatized at 30 °C was used for the determination of bromide in waters. The injection volume was set at 100 μL. A solution of 3.2 mM Na_2CO_3 and 1.0 mM $NaHCO_3$ at 0.7 mL/min was used as mobile phase.

2.3. Preparation of AgNCs

AgNCs were prepared in accordance with a procedure reported in the literature with slight modifications [39,40]. First, 100 μL of 0.2 M PEI, 50 μL of 1.0 mM HEPES and 95 μL of ultrapure water were blended under stirring with vortex for 2 min. Then, 125 μL of 0.1 M $AgNO_3$ was added and mixed under stirring for 2 min. After that, 5 μL of a 39 % (w/w) formaldehyde solution was added and the solution stirred for 2 min. Finally, the solution was heated at 70 °C for 10 min. The resulting AgNCs solution was stored at 4 °C for further use.

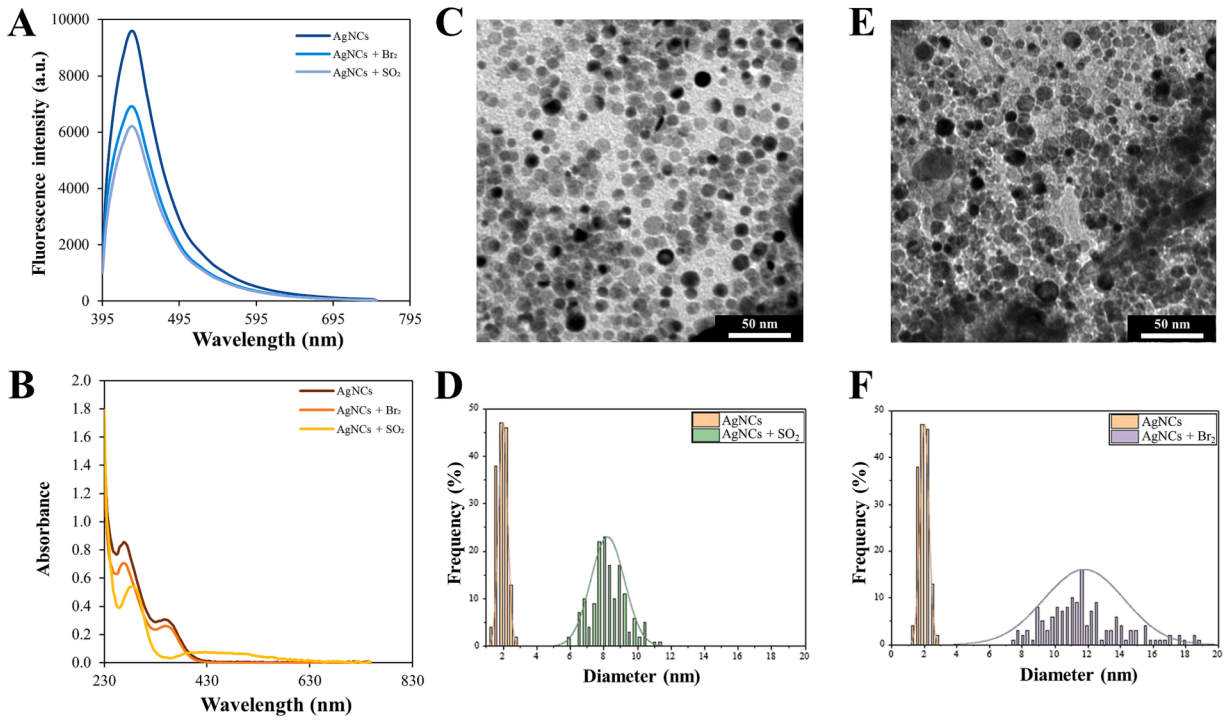

Fig. 1. Fluorescence spectra (A) and UV–visible spectra (B) of AgNCs in the presence and absence of SO_2 and Br_2. TEM images and size distribution histograms of AgNCs in the presence of SO_2 (C, D) and Br_2 (E, F).

2.4. Water and wastewater samples

Different water and wastewater samples were analyzed to evaluate the applicability of the assays developed in this work. Tap water was collected at the University of Vigo. Seawater samples were collected in two different areas of the Vigo Ria (NE Atlantic Coast). Synthetic wastewaters were prepared as described elsewhere [41,42]. In addition, urban and fishery wastewater samples from treatment plants were also used. In both cases, samples were collected both at the inlet and outlet of the treatment plants. The identity of the companies is not provided in agreement with a confidentiality clause. Water samples were stored in a refrigerator at 4 °C and analyzed within 24 h of sample collection.

2.5. Experimental procedures for sulfite and bromide determination

5 mL of aqueous solution (blank, standard solution or sample) is placed in a 20-mL amber vial containing a stir bar. A 5 μL-microdrop of AgNCs is deposited onto a circular Whatman 1PS substrate (1.8 cm diameter) placed over a PTFE-faced septum inside the screw cap. The vial is sealed with the drop exposed to the headspace above the sample, then 1.0 mL of a 1.0 M HCl (for *in situ* generation of SO_2) or 1.0 mL of a 0.1 M chloramine-T (for *in situ* generation of Br_2) is added to the sample and the solution is stirred at 1200 rpm for 30 min. Once the extraction has been completed, the cap with the AgNCs-containing microdrop is turned over and the fluorimetric and/or colorimetric smartphone-based assay is accomplished as described below.

Smartphone-based fluorimetric readout is carried out by placing the cap with the AgNCs microdrop in a dark cabinet and exposing it to UV radiation (365 nm) for digitization, with the ISO and the exposure value (EV) set at 400 and + 1.5, respectively. The analytical signal (mean color intensity in the B channel, Ic(B)) is obtained for the fluorimetric determination of bromide and sulfite at 5–500 μM concentration levels.

Alternatively, smartphone-based colorimetric readout is performed by digitization of the enriched AgNCs drop with a smartphone camera using a portable PULUZ photo studio lightbox to ensure constant lighting conditions. Ic(B) is thus obtained for the colorimetric determination of sulfite at 125–2000 μM concentration levels.

3. Results and discussion

3.1. Characterization of AgNCs

AgNCs were characterized using UV–vis spectrophotometry, fluorescence spectroscopy, TEM and XPS. As can be seen in the Fig. S1**A**, the UV–vis spectrum of AgNCs shows intense absorption bands at ca. 270 and 350 nm, the latter of which can be attributed to the oligomeric silver species [43]. Surface plasmon resonance bands are not observed in the range 400–500 nm, thus suggesting that large silver nanoparticles are not formed. Furthermore, the 3D fluorescence spectrum of AgNCs (Fig. S1**B**) shows that the highest analytical signal was obtained at an excitation/emission wavelength pair of 375/455 nm, in agreement with the previous literature [44]. Fig. S1**C** illustrates the TEM image of AgNCs and the corresponding particle size histogram, showing a size diameter of 2.0 ± 0.3 nm, in agreement with previous reports [39,45]. The survey XPS spectrum of AgNCs showed four peaks centered at 284, 398, 531 and 367 eV, corresponding to C, N, O and Ag, respectively (Fig. S1**D**). In addition, two binding energy peaks centered at 368.3 and 374.3 eV can be identified in the high resolution XPS spectrum of Ag3d (Fig. S1**E**). In addition, the Auger parameter obtained for AgNCs was 726. Both the Ag3d binding energy and the Auger parameter indicate that there is abundant silver in the metallic state, with an abundance equal to or greater than 80 % of all silver detected [46–48].

3.2. Recognition of Br_2 and SO_2 by AgNCs

In preliminary experiments we found that the optical properties of AgNCs microdrops were significantly modified in the presence of Br_2 and SO_2, unlike other volatiles such as hydrogen peroxide, iodine, nitrogen oxides and hydrogen sulfide. A number of experiments were conducted with the aim of shedding light on the responsiveness of AgNCs microdrops to both volatiles, the obtained results being observed in Fig. 1. The fluorescence emission spectrum of AgNCs was significantly

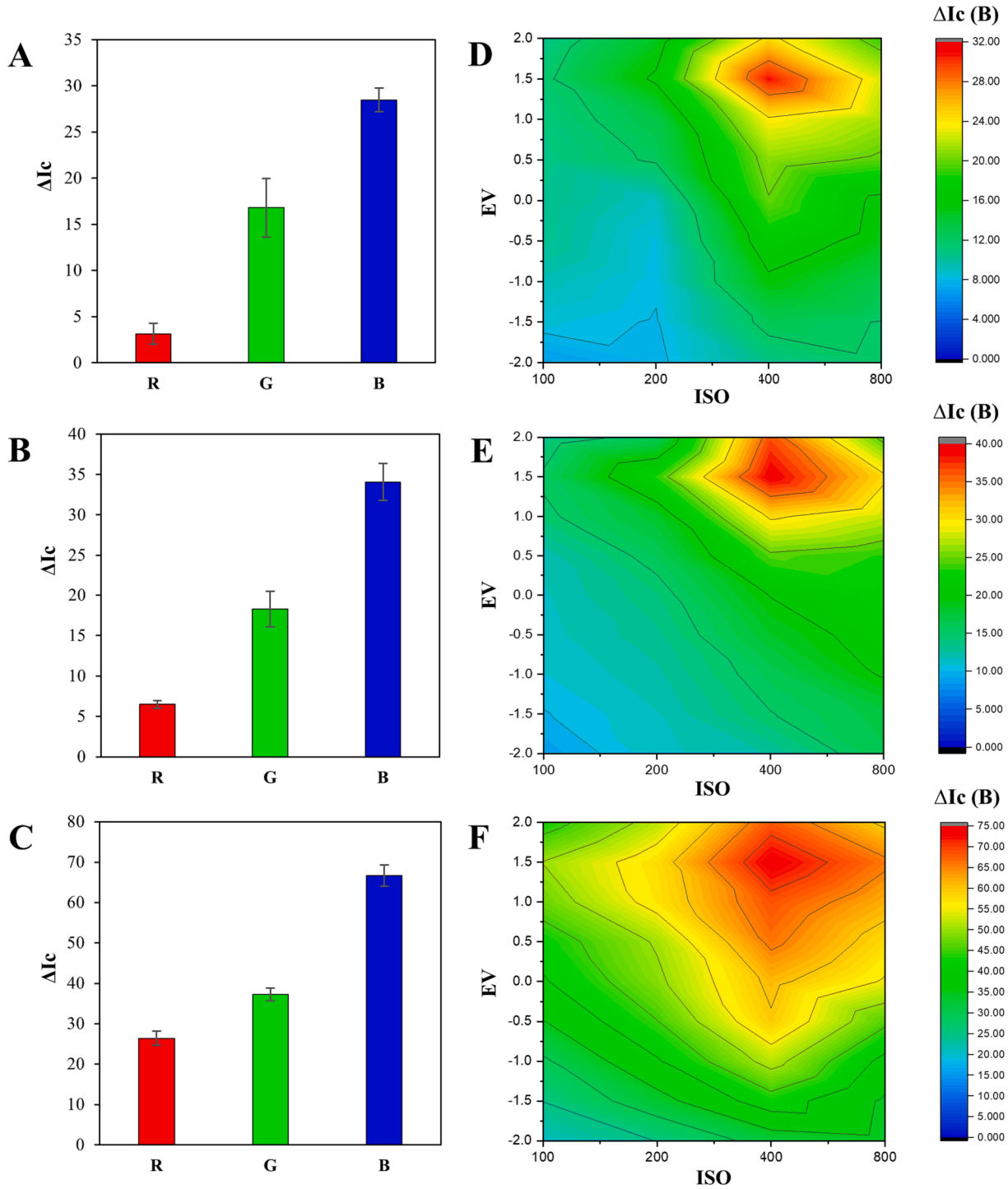

Fig. 2. Effect of color channels on the analytical response for the fluorimetric determination of bromide (A) and sulfite (B) and the colorimetric determination of sulfite (C); and effect of digitization parameters on the analytical response for the fluorimetric determination of bromide (D) and sulfite (E), and the colorimetric determination of sulfite (F).

quenched upon exposure to both volatiles (Fig. 1**A**), whereas the effect on the UV–visible spectrum of AgNCs was highly dependent on the volatile considered, as depicted in Fig. 1**B**. Thus, the UV–vis spectrum of AgNCs red-shifted in the presence of SO_2, showing a band at ca. 285 nm and a less intense and broader band at ca. 400–500 nm, leading to an obvious color change (from nearly colorless to yellowish/brown). Unlike SO_2, a slight decrease of the intensity of UV bands was produced in the presence of Br_2 without any further displacement of the bands being observed. In addition, the TEM images and size distribution histograms of AgNCs exposed to SO_2 and Br_2 are shown in Fig. 1**C-F**, respectively. An increase in both size and polydispersity was noticeable when AgNCs were exposed to SO_2 and Br_2, leading to diameter sizes of 8.2 ± 1.0 nm and 11.8 ± 2.5 nm, respectively.

On the basis of the above results and considering previous information reported in the literature, potential recognition mechanisms for Br_2 and SO_2 sensing are proposed herein. The different steps involved in the process, i.e., mass transfer of the volatiles at the gas-droplet interface, hydrolysis and ionization at the aqueous microdrop containing

AgNCs and subsequent interactions/reactions with AgNCs, should be taken into consideration.

Br_2 uptake by the AgNCs-containing microdrop is associated with partial hydrolysis of the halogen. Hypobromous acid and bromide ions are thus formed in the drop, and significant amounts of tribromide ions can also be formed in the presence of additional bromine [49]. Partial oxidation of AgNCs by HBrO can be hypothesized bearing in mind the high standard reduction potential of HBrO (E° HBrO/Br^-: +1.331 V), compared to that of Ag^0 (E° Ag^+/Ag^0: +0.7996 V) [50]. Formation of AgBr (K_{sp} 5.35 x 10^{-13}) [50] on the surface of AgNCs can then occur by reaction between the existing and released ionic Ag species and bromide ions [43], thus contributing to the formation of larger nanoparticles. Bromide ions have also been reported to induce oxidative etching with formation of AgBr-coated AgNCs followed by aggregation [43].

The collection of *in situ* formed SO_2 by the AgNCs-containing aqueous drop involves the hydration of SO_2 with formation of $SO_2(H_2O)_n$ clusters, followed by the formation of dissolved SO_2 and hydrolyzed species, including bisulfite or sulfite [51,52]. It is worth mentioning that the volatile uptake can be supported by the presence of the cationic polymer PEI in the microdrop. In fact, PEI has been found to be highly efficient for SO_2 removal, probably associated to the interactions between the ionic sulfur species and the abundant amine groups of PEI [53]. Thus, PEI-protected AgNCs could be disturbed in the presence of S(IV) species, leading to subsequent modifications of their size. In addition, the presence of ionic Ag species in the AgNCs microdrop could also contribute to the formation of larger nanoparticles. In fact, the formation of silver nanoparticles by reduction of Ag(I) into Ag^0 in the presence of SO_2 has been recently reported [54].

Based on the above results, AgNCs show much promise for the optical sensing of SO_2 and Br_2. Thus, AgNCs-containing microdrops have been exploited in this work for the development of colorimetric and/or fluorimetric smartphone-based assays for sulfite and bromide determination involving *in situ* generation of SO_2 and Br_2, respectively.

3.3. Optimization of experimental parameters

3.3.1. Digitization and image processing conditions

The effect of digitization and image processing conditions on the analytical response was initially assessed. The selection of the most appropriate RGB color channel was firstly performed. For this aim, microextraction experiments were conducted in the absence (blank) and presence of target analytes, and the resulting digital images of AgNCs-containing drops were processed to obtain the analytical response (i.e., mean color intensity difference (ΔIc) in each channel). As can be deduced from Fig. 2**A-C**, the B channel provides the maximum analytical response in all cases. These results were to be expected since, on the one hand, both volatiles led to the fluorescence quenching of blue-emitting AgNCs (emission wavelength, 455 nm) while, on the other hand, AgNCs underwent a color change from colorless to yellowish (i.e., close to the complementary color to blue) in the presence of relatively high concentrations of SO_2.

Two digitization settings, namely exposure value (EV) and ISO (International Organization for Standardization), were subsequently evaluated. EV combines shutter and aperture speed, whereas ISO indicates the camera's sensitivity and controls the amount of light it lets through. Both parameters have recently been shown to be of great importance in improving the sensitivity of smartphone-based detection approaches [29,55]. As can be observed in the Fig. 2**D-F**, the analytical response significantly increased with increasing both ISO and EV, showing the highest analytical response when the ISO and EV were set at 400 and + 1.5, respectively. These digitization conditions were therefore selected for subsequent studies.

3.3.2. Optimization of experimental parameters for sulfite and bromide determination

A screening-optimization strategy was subsequently employed for optimization of experimental conditions for determination of both sulfite and bromide. Thus, a Plackett-Burman design (PBD) was initially employed to assess which variables produced a significant effect on the analytical response at a given probability level, and subsequently, the significant variables were optimized by means of a central composite design (CCD). Seven experimental variables, namely AgNCs drop volume, extraction time, temperature, stirring rate, sample volume, NaCl concentration and concentration of derivatization agent (chloramine-T or HCl for bromide and sulfite, respectively) were included in the PBD for bromide and sulfite determination. In addition, four dummy variables were included in both cases to estimate the experimental error (Tables S1 and S2) [56,57]. Similar results were found for both bromide and sulfite determination (**Figure S2**). It can be deduced from the Pareto charts shown in the Figure that both extraction time and temperature showed significant effects on the analytical signals at a 95 % confidence level. Specifically, the extraction time was found to be the most significant parameter with a positive effect, as expected bearing in mind the key importance of this parameter in mass transfer processes. In contrast, temperature caused a significant negative effect on the analytical response. This depressive effect could be ascribed to the thermoresponsive nature of AgNCs, as reported in the literature [58].

Due to the observed effects, both variables, extraction time and temperature, were optimized using a CCD for both bromide and sulfite under the experimental conditions considered in Tables S3 and S4. As can be deduced from the Pareto chart showed in Fig. S3**A**, only the extraction time was found statistically significant for bromide determination. On the other hand, temperature, the interaction of both time and temperature and the quadratic effects were found not significant. Similar results were obtained for sulfite determination (Fig. S3**B**), with extraction time and its quadratic effect being the parameters that had a significant effect on the analytical response.

According to the results shown in the Pareto charts (**Figure S3**) and the response surfaces depicted in **Figure S4**, an extraction time of 30 min and a temperature of 20 °C were selected for determination of both anions. The remaining experimental conditions for the determination of bromide and sulfite were fixed as follows: AgNCs drop volume, 5 μL; stirring rate, 1200 rpm; sample volume, 5 mL; NaCl concentration, 0 % (w/v); and derivatization agent (chloramine-T or HCl) concentration, 0.1 M and 1.0 M, respectively.

3.4. Selectivity studies

Selectivity studies were carried out to evaluate the tolerance of the developed assays to the presence of potential interferences (**Table S5**). An interfering effect was considered significant when a variation beyond ± 10 % the analytical signal was observed. Under optimal conditions, the analytical response of bromide was not significantly affected in the presence of 3000 mM Cl^-, 1500 mM Mn(II), 1000 mM Co(II), 750 mM Mo(VI), 600 mM Cu(II), 530 mM Zn(II), 350 mM Ni(II), 300 mM COD (potassium hydrogen phthalate) and I^-, 250 mM EDTA, 125 mM $B(OH)_3$, 75 mM Ca(II), 70 mM Mg(II), 60 mM NH_4^+ and Se(IV), 55 mM $H_2PO_4^-$, 50 mM NO_3^- and K^+, 25 mM humic acid and 10 mM Fe(II). In addition, the determination of sulfite was not affected in the presence of the following species: 5000 mM Cl^-, 2500 mM Mn(II), 800 mM Zn(II) and Co(II), 650 mM COD (potassium hydrogen phthalate) and Mo(VI), 600 mM Ni(II), 500 mM Cu(II) and I^-, 350 mM EDTA, 160 mM $B(OH)_3$, 100 mM NO_3^- and K^+, 95 mM Ca(II), 75 mM $H_2PO_4^-$, 65 mM Se(IV), 60 mM Mg(II), 50 mM NH_4^+, and 25 mM Fe(II) and humic acid. The interference associated to Fe(II) was found to be alleviated by addition of NaF 10 mM. Under these conditions, Fe(II) did not interfere at a 100 mM level in the determination of both bromide and sulfite.

3.5. Analytical performance

The analytical characteristics of the assays were obtained under optimal conditions. As would be expected from previous studies [29,59],

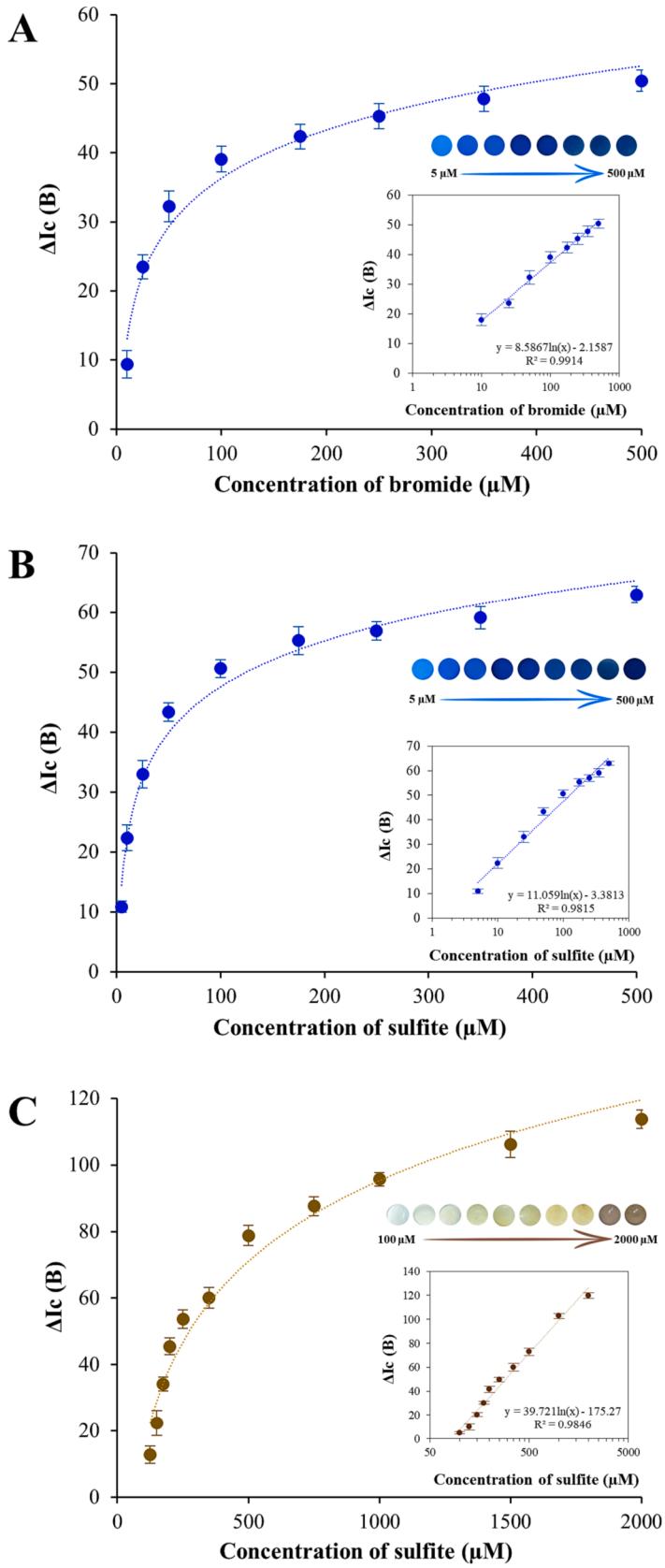

Fig. 3. Calibration curves for the fluorimetric determination of bromide (A) and sulfite (B), and for the colorimetric determination of sulfite (C).

Table 1
Analytical characteristics of methods involving optical detection for determination of bromide and sulfite.

Sensing material	Detection	LOD (μM)	Working range (μM)	Repeatability (%)	References
Bromide					
AgNPrs[a]	Colorimetric	0.13	0.31–25.03	3.29	[60]
AgTNPs[b]	Colorimetric	0.25	0.63–18.77	2.1–4.2	[61]
Phenol red and Chloramine-T	Colorimetric	40.3	0–125.2	–	[62]
AgNPs	Colorimetric	10	10–100000	–	[63]
TPCA[c]	Fluorimetric	0.07	0.38–1.88	7.8	[27]
AgNCs	Fluorimetric	1.5	5–500	5.1	This work
Sulfite					
CDs-AgNP/H_2O_2	Fluorimetric	3.02	20–200	0.3–6.2	[64]
Fe(II)-phenanthroline	Colorimetric	1.56	5–293	3.9–5.3	[65]
Formylazo dye (GJM 530)[d]	Colorimetric	220	220–8900	2.6	[66]
Bromocresol	Colorimetric	25	78.1–1406.2	2.2	[67]
AgNCs	Fluorimetric	1.1	5–500	5.9	This work
	Colorimetric	37.0	125–2000	5.6	

[c] AgNPrs silver nanoprisms.
[d] AgTNPs silver triangular nanoplates.
[b] 5-oxo-3,5-dihydro-2H-thiazolo[3,2-a]pyridine-7-carboxylic acid.
[a] 4-[4-(2- hydroxyethanesulfonyl)-phenylazo] − 2-formylnaphthalen-1-ol.

non-linear relationships between the analytical response, ΔIc(B) and the concentration of bromide and sulfite were obtained (Fig. 3**A-C**), showing a logarithmic dependency with the concentration, with correlation coefficients in the range 0.9645–0.9834. An improved fitting was achieved by means of the signal processing algorithm (1).

$$R = \Delta Ic(B)^{\alpha} \tag{1}$$

normalized as shown in (2).

$$Normalized\ Response = \frac{R - \min(R)}{\max(R) - \min(R)} \tag{2}$$

Reduced root-mean-square error (RMSE) values were obtained when α was set at 1.5–1.8, leading to residual plots where the data were randomly scattered around zero (**Figures S5-10**). Under these conditions, excellent correlation coefficients in the range 0.9944–0.9985 were obtained for the determination of both anions.

The limits of detection (LOD) and quantification (LOQ) of the smartphone-assisted fluorimetric assays for bromide and sulfite determination were calculated in accordance with the 3σ and 10σ criteria, respectively, being 1.5 and 3.6 μM for bromide and 1.1 and 2.9 μM for sulfite, respectively. The repeatability, expressed as relative standard deviation (RSD), was found to be 5.1 % and 5.9 % for bromide and sulfite, respectively (N = 8). In addition, the LOD and LOQ obtained for the colorimetric determination of sulfite were 37 and 94 μM, respectively, with a repeatability of 5.6 % (N = 8). In spite of its lower sensitivity, the smartphone-based colorimetric detection provides a wide working range (up to 2000 μM) and represents an effective and complementary alternative to fluorescence detection for sulfite determination.

A comparison of the analytical characteristics of the proposed assays with alternative approaches published in the literature for the determination of bromide and sulfite is provided (Table 1). It can be deduced that the proposed assays yielded comparable or even better LODs than those reported in the literature, showing acceptable precision. In addition, the reported assays are straightforward and the consumption of AgNCs per sample is almost negligible.

3.6. Application of the AgNCs-based assays

The applicability of the reported assays was evaluated by comparison with reference methods [10] for the determination of both bromide and sulfite in three water samples of increasing complexity. For those samples showing non-detectable contents of bromide and sulfite, the analysis of spiked samples was also carried out using both the proposed assays and the reference methods. As can be observed in the Tables S6 and S7, no significant differences occurred between the results obtained with the reported assays and the reference methods at a 95 % confidence level, since the experimental *t* values were lower than the corresponding critical *t* values. In addition, the reported assays were applied to the determination of bromide and sulfite in water samples, the obtained results being shown in Table 2. As can be observed, bromide was found at concentration levels of ca. 800–900 μM in seawater samples, in agreement with the concentration levels described in the literature [68]. In addition, bromide was quantified in the inlet flow of the fishery wastewater treatment plant with a content of 6.6 ± 0.3 μM. Bromide was also quantified in samples corresponding to the inlet and outlet flows of an urban wastewater treatment plant, with contents of 333.4 ± 16.8 μM and 35.9 ± 4.1 μM, respectively. Sulfite was found at concentration levels in the range of 8.3–55.4 μM in the wastewater samples, whereas it was below the LOD in the remaining samples. Recovery studies were carried out to evaluate the accuracy of the assays. Recovery values in the range 91 to 109 % were obtained in all cases. Thus, the matrix composition had no significant effect on the analytical results, allowing accurate results to be obtained. Furthermore, the proposed assays were applied to the monitoring of sulfite and bromide levels in a sulfite-mediated photoreduction process for bromate degradation. As can be

Table 2
Analytical results obtained by the application of the reported method for the determination of bromide and sulfite in water samples.

Sample	Bromide		Sulfite	
	Found (μM)	Recovery (%)[a]	Found (μM)	Recovery (%)[a]
Tap water	<LOD	104 ± 5	<LOD	93 ± 5
Seawater I	806 ± 42	94 ± 6	<LOD	108 ± 7
Seawater II	905 ± 32	92 ± 4	<LOD	107 ± 7
Synthetic wastewater I	<LOQ	97 ± 5	<LOD	96 ± 4
Synthetic wastewater II	<LOD	98 ± 7	<LOD	95 ± 6
Fishery wastewater (inlet)	6.6 ± 0.3	97 ± 8	26.3 ± 2.7	105 ± 9
Fishery wastewater (outlet)	<LOQ	92 ± 9	8.3 ± 0.9	106 ± 6
Urban wastewater (inlet)	333.4 ± 16.8	109 ± 8	55.4 ± 5.2	91 ± 7
Urban wastewater (outlet)	35.9 ± 4.1	91 ± 6	9.4 ± 0.8	94 ± 6

Results expressed as average value ± standard deviation (N = 3).
[a] Added concentration: 100 μM.

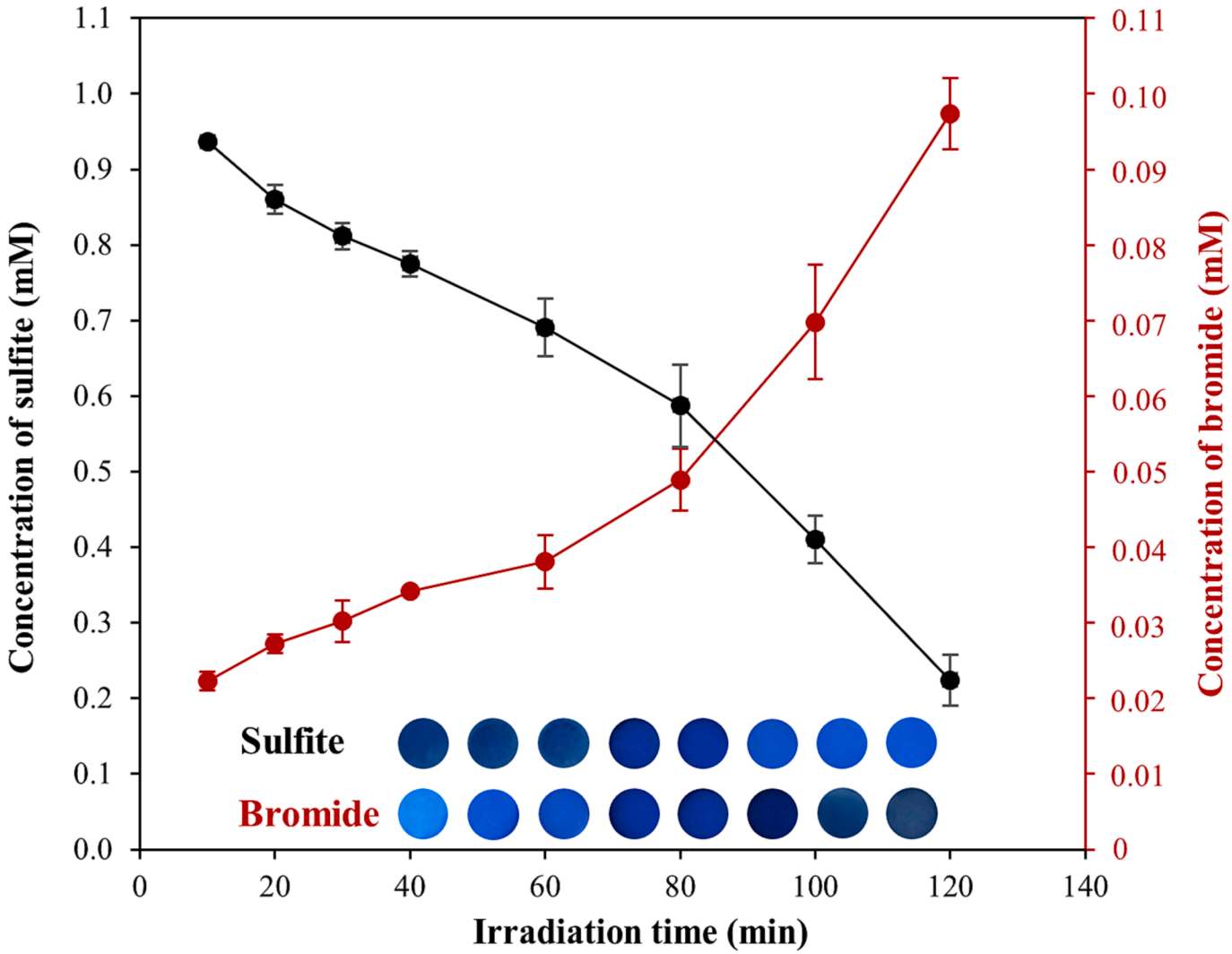

Fig. 4. Determination of bromide and sulfite in a water sample subjected to a sulfite-mediated photoreduction process for bromate degradation. Experimental conditions: Initial concentration of bromate, 100 μM; initial concentration of sulfite, 1.0 mM. The inset shows the appearance of AgNCs drops after analysis of samples treated by the ARP at increasing irradiation times.

observed in Fig. 4, the concentration of bromide increased continuously with increasing irradiation time. Thus, the concentration of bromate decreased accordingly, assuming a complete conversion of bromine species into bromide, as reported in the literature [49]. A quantitative conversion of bromate into bromide occurred when the aqueous solution was exposed to UV irradiation in the presence of sulfite for 2 h. Additionally, residual sulfite was determined in the aqueous phases by both the colorimetric and fluorimetric dual-modes. Sulfite concentration levels slightly decreased during the first 60 min, followed by an enhanced decline after this time. In addition, the much slower photodegradation of bromate in the absence of sulfite (9 % conversion after 120 min) was also verified by the application of the proposed assays [3].

4. Conclusions

This work reports on the applicability of AgNCs for in-drop Br_2 and SO_2 sensing. The luminescence quenching of AgNCs induced by both volatiles and the color transition (from nearly colorless to yellowish/brown) experienced only in the presence of SO_2 enabled the design of a nanosensor with fluorimetric readout for bromide and a dual-mode optical nanosensor for sulfite determination, respectively. The assays were characterized by their ease of operation and excellent selectivity. The smartphone-based digitization and image processing of AgNCs-containing microdrops was conveniently carried out without requiring drop manipulation. The assays developed in this work are expected to be valuable tools for monitoring purposes that will also support the development of advanced oxidation and reduction processes.

5. Novelty assessment

The present work reports, for the first time, on the assessment of silver nanoclusters as nanoprobes for integrated in-drop enrichment and smartphone-assisted detection with dual-signal readout for the determination of bromide and sulfite in aqueous matrices. As far as we are aware, this work represents the first report devoted to the determination of sulfite and bromide using a single optical nanosensor. The proposed assays are sensitive, straightforward, and affordable, and have demonstrated applicability in the analysis of aqueous samples of increasing complexity, including seawater and wastewater. In addition, the assays enabled the monitoring of sulfite and bromide in a sulfite-mediated photoreduction process for bromate degradation. The developed assays are envisaged to support the development of alternative advanced oxidation and reduction processes. Based on the above, we think the manuscript is appropriate for the journal ***Microchemical Journal***.

CRediT authorship contribution statement

Nerea Villarino: Methodology, Formal analysis, Investigation, Writing – review & editing. **Isela Lavilla:** Methodology, Data curation, Writing – review & editing. **Francisco Pena-Pereira:** Conceptualization, Validation, Supervision, Writing – original draft. **Carlos Bendicho:** Conceptualization, Writing – review & editing, Funding acquisition.

Declaration of competing interest

The authors declare that they have no known competing financial interests or personal relationships that could have appeared to influence the work reported in this paper.

Data availability

Data will be made available on request.

Acknowledgements

The corresponding authors thank the MCIN/ AEI / 10.13039/ 501100011033 / FEDER, UE (Project PID2022-136337OB-I00) for financial support. The CACTI facilities (University of Vigo) are also acknowledged. Funding for open access charge: Universidade de Vigo/ CISUG.

Appendix A. Supplementary data

Supplementary data to this article can be found online at https://doi.org/10.1016/j.microc.2023.109685.

References

[1] S. Dong, N. Masalha, M.J. Plewa, T.H. Nguyen, Toxicity of wastewater with elevated bromide and iodide after chlorination, chloramination, or ozonation disinfection, Environ. Sci. Technol. 51 (2017) 9297–9304, https://doi.org/10.1021/acs.est.7b02345.

[2] C. Watts, J. Sun, P.D. Jones, H. Peng, J.P. Giesy, Monthly variations of unregulated brominated disinfection by-products in chlorinated water are correlated with total bromine, Eco-Environ. Health 1 (2022) 147–155, https://doi.org/10.1016/j.eehl.2022.06.002.

[3] V.S.V. Botlaguduru, B. Batchelor, A. Abdel-Wahab, Application of UV–sulfite advanced reduction process to bromate removal, J. Water Process Eng. 5 (2015) 76–82, https://doi.org/10.1016/j.jwpe.2015.01.001.

[4] C.M. Morrison, S. Hogard, R. Pearce, A. Mohan, A.N. Pisarenko, E.R.V. Dickenson, U. von Gunten, E.C. Wert, Critical review on bromate formation during ozonation and control options for its minimization, Environ. Sci. Technol. (2023), https://doi.org/10.1021/acs.est.3c00538.

[5] M. Malakootian, S. Hamzeh, H. Mahmoudi-Moghaddam, An efficient electrochemical sensor for determination of sulfite in water and soft drinks based on Ce^{3+}-doped CuO nanocomposite, J. Food Compos. Anal. 113 (2022), 104716, https://doi.org/10.1016/j.jfca.2022.104716.

[6] L.E. Santos-Figueroa, C. Giménez, A. Agostini, E. Aznar, M.D. Marcos, F. Sancenõn, R. Martínez-Máñez, P. Amorõs, Selective and sensitive chromofluorogenic detection of the sulfite anion in water using hydrophobic hybrid organic-inorganic silica nanoparticles, Angew. Chemie - Int. Ed. 52 (2013) 13712–13716, https://doi.org/10.1002/anie.201306688.

[7] Regulation (EU) No 1169/2011 of the European Parliament and of the Council of 25 October 2011 on the provision of food information to consumers, amending Regulations (EC) No 1924/2006 and (EC) No 1925/2006 of the European Parliament and of the Council, and repealing Commission Directive 87/250/EEC, Council Directive 90/496/EEC, Commission Directive 1999/10/EC, Directive 2000/13/EC of the European Parliament and of the Council, Commission Directives 2002/67/EC and 2008/5/EC and Commission Regulation (EC) No 608/2004 Text with EEA relevance, 2011.

[8] Codex Alimentarius, General standard for food aditives – CODEX STAN 192, 1995, https://www.fao.org/fao-who-codexalimentarius/codex-texts/list-standards/en/ (accessed 26 October 2023).

[9] S. Wu, L. Shen, Y. Lin, K. Yin, C. Yang, Sulfite-based advanced oxidation and reduction processes for water treatment, Chem. Eng. J. 414 (2021), 128872, https://doi.org/10.1016/j.cej.2021.128872.

[10] A.D. Eaton, L.S. Clesceri, E.W. Rice, A.E. Greenberg, American Public Health Association, American Water Works Association and Water Environment Federation (APHA-AWWA-WEF), 4500-Br^- Bromide, in: Standard Methods for the Examination of Water and Wastewater, 21st ed., Washington DC, 2005.

[11] R. Zare-Dorabei, S. Boroun, M. Noroozifar, Flow injection analysis–flame atomic absorption spectrometry system for indirect determination of sulfite after on-line reduction of solid-phase manganese (IV) dioxide reactor, Talanta 178 (2018) 722–727, https://doi.org/10.1016/j.talanta.2017.10.012.

[12] K. Pandi, M. Sivakumar, S.-M. Chen, M. Sakthivel, G. Raghavi, T.-W. Chen, Y.-C. Liu, R. Madhu, Electrochemical synthesis of lutetium (III) hexacyanoferrate/poly(taurine) modified glassy carbon electrode for the sensitive detection of sulfite in tap water, J. Electrochem. Soc. 165 (2018) B469–B474, https://doi.org/10.1149/2.1171810jes.

[13] S.D. Rolle, C.H. Devillers, S. Fournier, O. Heintz, H. Gibault, D. Lucas, A glassy carbon electrode modified by a triply-fused-like Co(II) polyporphine and its ability for sulphite oxidation and detection, New J. Chem. 42 (2018) 8180–8189, https://doi.org/10.1039/c7nj04370h.

[14] F. Hissner, J. Mattusch, K. Heinig, Quantitative determination of sulfur-containing anions in complex matrices with capillary electrophoresis and conductivity detection, J. Chromatogr. A. 848 (1999) 503–513, https://doi.org/10.1016/S0021-9673(99)00458-6.

[15] A.M. Pisoschi, A. Pop, I. Gajaila, F. Iordache, R. Dobre, I. Cazimir, A.I. Serban, Analytical methods applied to the assay of sulfur-containing preserving agents, Microchem. J. 155 (2020), 104681, https://doi.org/10.1016/j.microc.2020.104681.

[16] M. Gorska, P. Pohl, Coupling of chemical vapor generation with atmospheric pressure glow discharge optical emission spectrometry generated in contact with flowing liquid electrodes for determination of Br in water samples, Microchem. J. 178 (2022), 107391, https://doi.org/10.1016/j.microc.2022.107391.

[17] R.E. Sturgeon, Detection of bromine by ICP-oa-ToF-MS following photochemical vapor generation, Anal. Chem. 87 (2015) 3072–3079, https://doi.org/10.1021/ac504747a.

[18] R. Wang, N. Wang, M. Ye, Y. Zhu, Determination of low-level anions in seawater by ion chromatography with cycling-column-switching, J. Chromatogr. A. 1265 (2012) 186–190, https://doi.org/10.1016/j.chroma.2012.09.086.

[19] E. Poboży, M. Trojanowicz, Application of capillary electrophoresis for determination of inorganic analytes in waters, Molecules 26 (2021) 6972, https://doi.org/10.3390/molecules26226972.

[20] H. Cunha-Silva, M.J. Arcos-Martinez, A disposable rhodium nanoparticle-modified screen-printed sensor for direct determination of bromide anions, Sensors Actuators B. Chem. 282 (2019) 603–608, https://doi.org/10.1016/j.snb.2018.11.108.

[21] F. Pena-Pereira, A. García-Figueroa, I. Lavilla, C. Bendicho, Nanomaterials for the detection of halides and halogen oxyanions by colorimetric and luminescent techniques: a critical overview, TrAC - Trends Anal. Chem. 125 (2020), 115837, https://doi.org/10.1016/j.trac.2020.115837.

[22] K. Grudpan, S.D. Kolev, S. Lapanantnopakhun, I.D. McKelvie, W. Wongwilai, Applications of everyday IT and communications devices in modern analytical chemistry: a review, Talanta 136 (2015) 84–94, https://doi.org/10.1016/j.talanta.2014.12.042.

[23] L.F. Capitán-Vallvey, N. López-Ruiz, A. Martínez-Olmos, M.M. Erenas, A.J. Palma, Recent developments in computer vision-based analytical chemistry: a tutorial review, Anal. Chim. Acta. 899 (2015) 23–56, https://doi.org/10.1016/j.aca.2015.10.009.

[24] T. Ozer, C. McMahon, C.S. Henry, Advances in paper-based analytical devices, Annu. Rev. Anal. Chem. 13 (2020) 85–109, https://doi.org/10.1146/annurev-anchem-061318- 114845.

[25] R. Sun, Y. Li, T. Du, Y. Qi, Recent advances in integrated dual-mode optical sensors for food safety detection, Trends Food Sci. Technol. 135 (2023) 14–31, https://doi.org/10.1016/j.tifs.2023.03.013.

[26] F. Pena-Pereira, I. Lavilla, I. de la Calle, V. Romero, C. Bendicho, Detection of gases and organic vapors by cellulose-based sensors, Anal. Bioanal. Chem. 415 (2023) 4039–4060, https://doi.org/10.1007/s00216-023-04649-z.

[27] L. Placer, I. Lavilla, F. Pena-Pereira, C. Bendicho, Bromine speciation by a paper-based sensor integrated with a citric acid/cysteamine fluorescent probe and smartphone detection, Sensors Actuators B Chem. 358 (2022), 131499, https://doi.org/10.1016/j.snb.2022.131499.

[28] F. Pena-Pereira, L. Villar-Blanco, I. Lavilla, C. Bendicho, Test for arsenic speciation in waters based on a paper-based analytical device with scanometric detection, Anal. Chim. Acta. 1011 (2018) 1–10, https://doi.org/10.1016/j.aca.2018.01.007.

[29] N. Villarino, F. Pena-Pereira, I. Lavilla, C. Bendicho, Waterproof cellulose-based substrates for in-drop plasmonic colorimetric sensing of volatiles: application to acid-labile sulfide determination in waters, ACS Sensors. 7 (2022) 839–848, https://doi.org/10.1021/acssensors.1c02585.

[30] N. Villarino, I. Lavilla, F. Pena-Pereira, C. Bendicho, Droplet-based luminescent sensor supported onto hydrophobic cellulose substrate for assessing fish freshness following smartphone readout, Food Chem. 424 (2023), 136475, https://doi.org/10.1016/j.foodchem.2023.136475.

[31] D. Li, H. Duan, Y. Ma, W. Deng, Headspace-sampling paper-based analytical device for colorimetric/surface-enhanced Raman scattering dual sensing of sulfur dioxide in wine, Anal. Chem. 90 (2018) 5719–5727, https://doi.org/10.1021/acs.analchem.8b00016.

[32] Z. Xia, D. Li, W. Deng, Identification and detection of volatile aldehydes as lung cancer biomarkers by vapor generation combined with paper-based thin-film microextraction, Anal. Chem. 93 (2021) 4924–4931, https://doi.org/10.1021/acs.analchem.0c05348.

[33] Y. Hou, C. Lv, W. Liu, Y. Guo, Y. Jin, B. Li, Y. Zhang, Y. Liu, In situ synthesis of copper metal-organic framework on paper-based device for dual-mode detection of volatile sulfur compounds in exhaled breath, Sensors Actuators B Chem. 352 (2022), 131008, https://doi.org/10.1016/j.snb.2021.131008.

[34] J. Li, J.J. Zhu, K. Xu, Fluorescent metal nanoclusters: From synthesis to applications, TrAC - Trends Anal. Chem. 58 (2014) 90–98, https://doi.org/10.1016/j.trac.2014.02.011.
[35] L. Zhang, E. Wang, Metal nanoclusters: new fluorescent probes for sensors and bioimaging, Nano Today. 9 (2014) 132–157, https://doi.org/10.1016/j.nantod.2014.02.010.
[36] S. Qian, Z. Wang, Z. Zuo, X. Wang, Q. Wang, X. Yuan, Engineering luminescent metal nanoclusters for sensing applications, Coord. Chem. Rev. 451 (2022), 214268, https://doi.org/10.1016/j.ccr.2021.214268.
[37] Y. Pan, Z. Han, S. Chen, K. Wei, X. Wei, Metallic nanoclusters: From synthetic challenges to applications of their unique properties in food contamination detection, Coord. Chem. Rev. 478 (2023), 214964, https://doi.org/10.1016/j.ccr.2022.214964.
[38] C.A. Schneider, W.S. Rasband, K.W. Eliceiri, NIH image to ImageJ: 25 years of image analysis, Nat. Methods. 9 (2012) 671–675, https://doi.org/10.1038/nmeth.2089.
[39] N. Zhang, F. Qu, H.Q. Luo, N.B. Li, Sensitive and selective detection of biothiols based on target-induced agglomeration of silver nanoclusters (2013) 214–218, https://doi.org/10.1016/j.bios.2012.10.090.
[40] H. Xu, K.S. Suslick, Water-soluble fluorescent silver nanoclusters, Adv. Mater. 22 (2010) 1078–1082, https://doi.org/10.1002/adma.200904199.
[41] M. Adnan, S.J. Khan, K. Manzoor, N.P. Hankins, Performance evaluation of fertilizer draw solutions for forward osmosis membrane bioreactor treating domestic wastewater, Process Saf. Environ. Prot. 127 (2019) 133–140, https://doi.org/10.1016/j.psep.2019.05.006.
[42] P. Falås, R. Juárez, L.A. Dell, S. Fransson, S. Karlsson, M. Cimbritz, Microbial bromate reduction following ozonation of bromide-rich wastewater in coastal areas 841 (2022), 156694, https://doi.org/10.1016/j.scitotenv.2022.156694.
[43] F. Qu, N.B. Li, H.Q. Luo, Polyethyleneimine-templated Ag nanoclusters: a new fluorescent and colorimetric platform for sensitive and selective sensing halide ions and high disturbance-tolerant recognitions of iodide and bromide in coexistence with chloride under condition of high ionic strength, Anal. Chem. 84 (2012) 10373–10379, https://doi.org/10.1021/ac3024526.
[44] J.R. Zhang, A.L. Zeng, H.Q. Luo, N.B. Li, Fluorescent silver nanoclusters for ultrasensitive determination of chromium(VI) in aqueous solution, J. Hazard. Mater. 304 (2016) 66–72, https://doi.org/10.1016/j.jhazmat.2015.10.036.
[45] D. Xu, Q. Wang, T. Yang, J. Cao, Q. Lin, Z. Yuan, L. Li, Polyethyleneimine capped silver nanoclusters as efficient antibacterial agents, Int. J. Environ. Res. Public Health. 13 (2016) 334, https://doi.org/10.3390/ijerph13030334.
[46] B. Samai, S. Chall, S.S. Mati, S.C. Bhattacharya, Role of silver nanoclusters in the enhanced photocatalytic activity of cerium oxide nanoparticles, Eur. J. Inorg. Chem. 2018 (2018) 3224–3231, https://doi.org/10.1002/ejic.201800230.
[47] Z. Yuan, N. Cai, Y. Du, Y. He, E.S. Yeung, Sensitive and selective detection of copper ions with highly stable polyethyleneimine-protected silver nanoclusters, Anal. Chem. 86 (2014) 419–426, https://doi.org/10.1021/ac402158j.
[48] C. Wang, J. Wu, K. Jiang, M.G. Humphrey, C. Zhang, Stable Ag nanoclusters-based nano-sensors: Rapid sonochemical synthesis and detecting Pb^{2+} in living cells, Sensors Actuators B Chem. 238 (2017) 1136–1143, https://doi.org/10.1016/j.snb.2016.07.090.
[49] Q. Xiao, T. Wang, S. Yu, P. Yi, L. Li, Influence of UV lamp, sulfur(IV) concentration, and pH on bromate degradation in UV/sulfite systems: mechanisms and applications, Water Research. 111 (2017) 288–296, https://doi.org/10.1016/j.watres.2017.01.018.
[50] R.C. Weast, CRC Handbook of Chemistry and Physics, 67th ed., CRC Press, Boca Ratón, Fl, 1986.
[51] S.T. Moin, T.S. Hofer, B.R. Randolf, B.M. Rode, An ab initio quantum mechanical charge field molecular dynamics simulation of hydrogen peroxide in water, Comput. Theor. Chem. 980 (2012) 3379–3386, https://doi.org/10.1016/j.comptc.2011.11.006.
[52] E.S. Shamay, N.A. Valley, F.G. Moore, G.L. Richmond, Staying hydrated: the molecular journey of gaseous sulfur dioxide to a water surface, Phys. Chem. Chem. Phys. 15 (2013) 6893–6902, https://doi.org/10.1039/c3cp50609f.
[53] W. Bo, H. Li, J. Zhang, X. Song, J. Hu, C. Liu, Absorption of sulfur dioxide from simulated flue gas by polyethyleneimine-phosphoric acid solution, Environ. Technol. (united Kingdom) 37 (2016) 3062–3070, https://doi.org/10.1080/21622515.2016.1175513.
[54] Z. Hao, F. Li, R. Liu, X. Zhou, Y. Mu, V.K. Sharma, J. Liu, G. Jiang, Reduction of ionic silver by sulfur dioxide as a source of silver nanoparticles in the environment, Environ. Sci. Technol. 55 (2021) 5569–5578, https://doi.org/10.1021/acs.est.0c08790.
[55] Y. Fan, J. Li, Y. Guo, L. Xie, G. Zhang, Digital image colorimetry on smartphone for chemical analysis: a review, Measurement 171 (2021), 108829, https://doi.org/10.1016/j.measurement.2020.108829.
[56] Y. Vander Heyden, K. Luypaert, C. Hartmann, D.L. Massart, J. Hoogmartens, J. De Beer, Ruggedness tests on the high-performance liquid chromatography assay of the United States Pharmacopeia XXII for tetracycline hydrochloride. a comparison of experimental designs and statistical interpretations, Anal. Chim. Acta. 312 (1995) 245–262, https://doi.org/10.1016/0003-2670(95)00221-K.
[57] Y. Vander Heyden, C. Hartmann, D.L. Massart, L. Michel, P. Kiechle, F. Erni, Ruggedness tests for a high-performance liquid chromatographic assay: comparison of an evaluation at two and three levels by using two-level Plackett-Burman designs, Anal. Chim. Acta. 316 (1995) 15–26, https://doi.org/10.1016/0003-2670(95)00349-5.
[58] F. Qu, Q. Li, J. You, Fluorescent silver nanoclusters capped by polyethyleneimine with different molecular weights: universal synthesis and application as a temperature sensor, J. Lumin. 177 (2016) 133–138, https://doi.org/10.1016/j.jlumin.2016.04.040.
[59] C.C. Hsu, Y.Y. Chao, S.W. Wang, Y.L. Chen, Polyethylenimine-capped silver nanoclusters as fluorescent sensors for the rapid detection of ellagic acid in cosmetics, Talanta 204 (2019) 484–490, https://doi.org/10.1016/j.talanta.2019.06.047.
[60] K. Phoonsawat, W. Dungchai, Highly sensitive, selective and naked-eye detection of bromide and bromate using distance–based paper analytical device, Talanta 221 (2021), 121590, https://doi.org/10.1016/j.talanta.2020.121590.
[61] M.O. Gorbunova, M.S. Garshina, M.S. Kulyaginova, V.V. Apyari, A.A. Furletov, A. V. Garshev, S.G. Dmitrienko, Y.A. Zolotov, A dynamic gas extraction-assisted paper-based method for colorimetric determination of bromides, Anal. Methods. 12 (2020) 587–594, https://doi.org/10.1039/c9ay02640a.
[62] L.J. Loh, G.C. Bandara, G.L. Weber, V.T. Remcho, Detection of water contamination from hydraulic fracturing wastewater: a μPAD for bromide analysis in natural waters, Analyst 140 (2015) 5501–5507, https://doi.org/10.1039/c5an00807g.
[63] S.H. Kim, H.C. Woo, M.H. Kim, Solid-phase colorimetric sensing probe for bromide based on a tough hydrogel embedded with silver nanoprisms, Anal. Chim. Acta. 1131 (2020) 80–89, https://doi.org/10.1016/j.aca.2020.07.035.
[64] Y. He, Y. Wang, S. Wang, Carbon dot and silver nanoparticle-based fluorescent probe for the determination of sulfite and bisulfite via inner-filter effect and competitive redox reactions, Microchim. Acta. 190 (2023) 190, https://doi.org/10.1007/s00604-023-05782-3.
[65] C. Khamkhajorn, S. Pencharee, J. Jakmunee, N. Youngvises, Smartphone-based colorimetric method for determining sulfites in wine using a universal clamp sample holder and microfluidic cotton swab-based analytical device, Microchem. J. 174 (2022), 107055, https://doi.org/10.1016/j.microc.2021.107055.
[66] M.J. Arroyo, I. de Orbe-Payá, M. Ortega-Muñoz, J. Vilar-Tenorio, D. Gallego, G. J. Mohr, L.F. Capitán-Vallvey, M.M. Erenas, Capillary microfluidic platform for sulfite determination in wines, Sensors Actuators B Chem. 359 (2022), 131549, https://doi.org/10.1016/j.snb.2022.131549.
[67] G.M. Fernandes, D.N. Barreto, A.D. Batista, J.F. da Silveira Petruci, A fully integrated 3D printed platform for sulfite determination in beverages via gas diffusion membrane extraction and digital video treatment, Food Chem. 406 (2023), 135094, https://doi.org/10.1016/j.foodchem.2022.135094.
[68] Y. Chen, R.G. Compton, A bespoke reagent-free amperometric bromide sensor for seawater, Talanta 253 (2023), 124019, https://doi.org/10.1016/j.talanta.2022.124019.